TEARING INSTABILITY AND THE DEVELOPMENT OF VOIDS IN A LOW-ALLOY STEEL

C. Q. Zheng* and J. C. Radon**

*North Western Polytechnical University, Xi'an, People's Republic of China
**Imperial College, London SW7 2BX, England

ABSTRACT

Ductile fracture tests and static tensile tests were performed on a low-alloy steel BS 4360-50D used extensively in the construction of the large North Sea oil rigs. The tearing instability concept was applied to investigate the fracture process. Ductile fracture occurring by the formation, growth and coalescence of voids around the inclusions was described.

Two specific values of plastic strain were noted, namely, $\varepsilon_p \approx 0.22$, corresponding to the strain hardening exponent n near the range of necking when a large number of voids suddenly formed, and $\varepsilon_p \approx 0.97$, corresponding to the instability strain, which is about 90 per cent of the fracture strain. At this strain the voids were coalescing and ligaments and partition walls began to fracture.

A linear semi-logarithmic relationship between the relative void volume and the plastic strain was established for smooth cylindrical tensile specimens in the range of necking. Finally, a static toughness value of $J = 293$ N/mm was derived; this compares favourably with experimental results.

KEYWORDS

Tearing modulus; J-integral; ductile fracture; development of voids; instability strain.

INTRODUCTION

Structural safety of very large frameworks such as offshore oil platforms, is of fundamental importance and at the present time a considerable amount of attention is being given to the subject of their construction. The reliability analysis has recently been applied in detail to all designs of oil rigs and in particular to possible fatigue failures. It is well known that these types of large structures are statically and dynamically indeterminate. Consequently, one of the important factors is the redistribution of forces after a partial collapse which can occur only when a sufficient deformation capacity of the structural members is available.

This force redistribution process is of basic importance for reliable and efficient engineering design. It seems clear that the deformation capacity of any structural member is closely related to the stress-strain properties of the material used. Thus a detailed investigation of these properties and their effect on the mechanical behaviour of the structure is necessary.

A low-alloy steel BS4360-50D is widely used for the construction of oil rigs and a preliminary investigation of some of its basic properties has been reported (1). This present paper describes three specific aspects of the tensile fracture: namely, the low strain rate tensile test; the void formation process during the local necking; and the application of the tearing instability concept for tensile cracks under fully plastic conditions.

TEARING MODULUS

It is a common practice to determine the tensile properties of a material using round bar test-pieces, such as in this investigation, according to the standard BS18 (1971). Static tensile tests were performed at a loading rate of $0.05\ mm/min$ on cylindrical specimens, $d_o = 11.28\ mm$. The specimens were manufactured from a 50 mm thick plate with their axes parallel to RD. The testing procedure and the results obtained are described in (1). The necking process is of particular interest here.

After the general yielding and at the beginning of the necking the strain hardening coefficient n reached the value of 0.22. On completion of the necking, the value of n increased to 0.27. The ultimate failure of the specimen was characterised by gross yielding in the gauge length. As discussed later, the voids formed around the inclusions mostly in the necked region. Some voids nucleated before reaching the maximum load, but the majority formed at and after the maximum load. In order to further develop the present understanding of the fracture, the tearing instability criterion (2,4) was applied.

The concept of tearing modulus, T, has been developed on the basis of the J-integral resistance curve and the two non-dimensional quantities, $T_{material}$ and $T_{applied}$. The value of T_{mat} represents all intrinsic properties of the material, while T_{app} refers to the geometric configuration of the specimen. Both quantities may be defined as follows:

$$T_{mat} = \frac{E}{\sigma_o^2} \frac{dJmat}{da} \qquad (1)$$

$$T_{app} = \frac{4Ld}{D^2} \qquad (2)$$

Here the term T_{app} represents the geometry of a centre-cracked (a penny shape crack) round test-piece or that of a notched round bar. The deformation condition of stability of crack growth is given by the following inequalities:

$$T_{mat} > T_{app} \ldots\ldots\ldots \text{ stable condition} \qquad (3)$$

$$T_{mat} < T_{app} \ldots\ldots\ldots \text{ unstable condition} \qquad (4)$$

In these expression: E is Young's modulus ($2.133 \times 10^5\ MPa$ for steel), σ_o is true fracture stress or flow stress (4). a is the relevant crack or flaw size for the stability analysis. J_{mat} is the value of J-integral following the material resistance curve. L is the effective specimen length, adjusted

for the compliance of the machine, grips and the button ends of the specimen. D and d are the gauge diameter and the crack length of the specimen respectively.

At the beginning of the necking process no internal crack in the body of the specimen gauge length was assumed,

$$\text{i.e.} \qquad d = 2a \simeq 0. \qquad (5)$$

Therefore:-

$$T_{app} \simeq 0 \qquad (6)$$

Using the appropriate experimental data for 50D steel we obtain

$$T_{mat} = 35.8 \qquad (7)$$

The following values (1,3) were applied:

$$\frac{dJ}{da} = 225\ MPa$$

$$\sigma_o = 1158\ MPa$$

Comparing equations (6) and (7) it is seen that

$$T_{mat} > T_{app}$$

and consequently, according to equation (3) the condition is stable.

Now considering the point of failure, it will be realised that the situation is different. Four necking tests were performed and the respective values of T_{mat}, T_{app} recorded, resulting in:

$$T_{mat} < T_{app}$$

this inequality corresponds with the process of unstable deformation, equation (4).

The change in the degree of stability involved in this process may be described as follows. The formation of the neck started at, or close before reaching the maximum load P_{max}, which in the present static monotonic tests corresponds to the stress $\sigma_{max} = 550\ MPa$. On reaching this load the necking could be easily observed on the surface of the specimen. At the same time a microflaw (a void) developed in the centre of the specimen neck. It was assumed that this microflaw would begin to grow only after a certain amount of deformation of the specimen. At the same time, T_{app}, which until now was near zero, started increasing. The formation and the gradual growth of the microflaw was a stable process. Ideally it could be expected that the microflaw may develop into a penny-shaped crack. It is suggested that as the crack d is growing, the value of T_{app} is increasing as well. With the increasing T_{app}, the value of T_{mat} is decreasing, leading to the critical point where $T_{app} = T_{mat}$, followed by $T_{app} > T_{mat}$ and resulting in the complete separation.

FORMATION OF VOIDS

Basically, the micromechanism of ductile fracture takes place in three distinct stages namely: 1) nucleation, or initiation of voids; 2) growth of

voids; and 3) coalescence of voids leading to final fracture (separation). It has been known for some time that the cohesion of small second phase particles with the matrix is very strong and this applies to nearly all engineering materials. However, the cohesion of larger second phase particles with the matrix is substantially weaker. Consequently, after a certain amount of matrix deformation, some larger particles may crack or fracture and this process will be followed by the formation of microvoids. In low-alloy steels of the type discussed here, the main void initiating particles are usually MnS and CaS, etc. Due to the rolling processes involved in the manufacture these inclusions are in general ellipsoidal, but as a consequence of the processing they may often be very irregular and also flattened in the transverse directions. This rather complicated geometry of the inclusions strongly affects the deformation behaviour of the material and the prediction of fracture is not an easy task.

In order to investigate the fracture process in more detail the tests were interrupted at convenient intervals. Therefore, in addition to the standard tensile tests described in (1), further tests were performed with suitable interruptions during the yielding process, before necking, during necking, after necking but before instability and finally, at the moment of separation. On the completion of these tests all the specimens were split along their longitudinal axes in a liquid nitrogen bath and some of them sectioned by the milling machine and subsequently polished and etched using 2% Nital. The microstructure was studied with the help of the scanning electron microscope JSM-T200 and the Link Systems Model 860. The following figures show some typical formations and growth of voids found in 50D steel:-

Fig. 1a) A spheroidal inclusion with very small voids.

Fig. 1b) A typical ellipsoidal void with a spheroidal inclusion ($\varepsilon_p \approx 0.8$).

Fig. 1c) A large number of voids completely enveloping small inclusions.

Some voids nucleated transverse to the loading direction Fig. 2, $(CaO)_x\ (Al_2O_3)_y$ in the form of large hexagonal particles.

The void nucleation process was observed typically at the following inclusions: MnS (angular shape, mostly about 10 to 50 μm large). Here the void nucleation began at $\varepsilon_p < 0.15$.

Other inclusions, observed in decreasing size, were as follows:

CaS ($\sim 25\ \mu m$).

$CaO \cdot MgO \cdot SiO_2$ (15 to 25 μm).

$Ca_x \cdot (Al_2O_3)_y \cdot SiO_2$ ($\sim 25\ \mu m$).

$(CaO)_x \cdot (Al_2O_3)_y$ (Hexagonal, 15 - 45 μm).

$(CaO)_x \cdot (Al_2O_3)_y$ (very irregular shape, 15 μm).

SiO_2 ($\sim 8 \mu m$).

$MnO \cdot FeO$ (3 - 9 μm).

$(MgO)_x \cdot (Al_2O_3)_y \cdot MnO$ (2 - 4 μm).

Mixtures of MnS and Al_2O_3 ($\sim 4\ \mu m$).

Cu particles ($\sim 1.3\ \mu m$).

MnS in the shape of very small spheres ($\sim 0.7\ \mu m$).

It was noted that the process of void formation consisted of two parts: The primary nucleation started during the yielding of the material. Only a few voids were observed before necking, but their number increased at $\varepsilon_p \approx 0.15 - 0.22$. Contrary to the primary nucleation, the formation and growth of the secondary voids, around the submicron particles was in sudden bursts and fast. It was thought that this rapid growth was achieved by the increasing strain. In the final phase, voids rapidly enlarged and coalesced as the strain reached the instability point. Thus the actual crack formation process was found to be dependent on the instability strain.

The formation of primary voids occurred mostly around large inclusions, such as MnS, CaS, $CaO.Al_2O_3$, or $CaO.MgO.SiO_2$, Fig. 2. The secondary voids were adjacent to the submicron inclusions and, exceptionally, close to the medium size inclusions.

Figure 3 shows the relationship between the relative void volume V_v and plastic strain ε_p.

The average value of the slope in the strain region limited by $(0.15 < \varepsilon_p < 1.0)$ is

$$S = \frac{ln(V_v/V_o)}{\bar{\varepsilon}_p - \bar{\varepsilon}_o} \simeq 2.2 \qquad (8)$$

which represents the value of $(ln\ V_v/V_o)/(\varepsilon_p - \varepsilon_o)$ being nearly constant for smooth cylindrical tensile specimens after necking within the range of $\frac{\sigma_m}{\bar{\sigma}} \approx 0.34$ to 0.74.

Two specific values of plastic strain are of interest. Firstly, at ε_p of 0.22 a large number of voids suddenly formed, increasing substantially the relative void volume. We consider this strain being a typical value corresponding to the beginning of the necking process. The second volume increase occurred at ε_p equal 0.97 which is the instability strain. At this strain the voids were coalescing and the ligaments and partition walls fractured.

THE INSTABILITY STRAIN

In the previous paper (1) it was shown that the instability strain ε_i was invariably lower than the true fracture strain. Two plates of 50D steel of different proveniance were used for the instability tests giving slightly different strain hardening exponents. Consequently two groups of tests were performed; in the first group, the instability strain ε_i being equal to 0.97 i.e. 90% of the true fracture strain amounting to 1.08. In the second group both the mean instability strain and the true fracture strain reached higher values, but their ratio was still equivalent to 90%.

Rice (15) suggested that the instability strain may be expressed as

$$\varepsilon_i = \sqrt{(1 + 3n)\ (1 - n)/3} \qquad (9)$$

where n is the strain hardening exponent. For our steel 50D, the value of n at instability is 0.27 and using equation (9) we obtain $\varepsilon_i = 0.664$. This is much lower than the experimental value mentioned above. Similar, but again rather low results were obtained using the Hutchinson's (6) analysis. It should be noted that the strain hardening exponent will influence the ε_i only marginally. For example, for a very low value of

$n = 0.15$, ε_i was 0.64, but for the increased n of 0.22, corresponding to the situation just before necking, ε_i increased only to 0.66, still very different from the experimental value. Consequently Equation (9) may need some adjustments. Also, in the true strain range $\varepsilon_p = 0.5$ to 0.6 a number of strings of voids and their coalescence in the loading direction was observed. Because of the low strain and unexpected direction of string formation, this phenomenon warrants additional investigation.

THE CORRELATION OF TENSILE PROPERTIES AND FRACTURE TOUGHNESS

The relationship between the toughness and some other properties of materials has been investigated by many workers. It is now generally accepted that a correlation between tensile properties and fracture parameters exists. For example, Hahn and Rosenfield (7) suggested that the toughness K_{1c} may be expressed as

$$K_{1c} = \left(\frac{2}{3} E \sigma_y \, n^2 \, \varepsilon_f\right)^{\frac{1}{2}} \qquad (10)$$

This relationship has been successfully used for high strength alloy steels; it is also suitable for the 50D steel. It is customary to express J_{1c} as follows:-

$$J_{1c} = \frac{K_{1c}^2}{E} (1 - \nu^2) \qquad (11)$$

and applying equation (10) we obtain (adjusted for SI units)

$$J_{1c} = \left(\frac{2}{3} (1-\nu^2) \, \sigma_y \, \varepsilon_f\right) 25.4 \qquad (12)$$

Using the data from (1, 8) we finally obtain

$$J_{1c} = 293 \ N/mm$$

Two sets of experiments, using CT-specimens made from two plates, as supplied, were performed according to ASTM E813-81. The following results were obtained:

For the first group : $J_{1c} = 289 \ N/mm$

For the second group : $J_{1c} = 271 \ N/mm$

giving a mean value : $J_{1c} = 280 \ N/mm$

The difference between the two series of tests amounts to 5%, which is considered satisfactory.

CONCLUSIONS

The tearing instability concept and the tearing modulus criterion were used to investigate the tensile deformation of the low-alloy steel BS4360-50D in the laboratory air at 20°C, applying a loading rate of $0.05 mm/min$. The nucleation of voids was studied in detail.

1. The primary voids nucleated around larger (> 10 μm) inclusions, such as MnS, CaS and $CaO.Al_2O_3.SiO_2$. At much higher strains an additional nucleation of secondary voids occured even at very small inclusions (< 1 μm).

2. A linear semi-logarithmic relationship between relative void volume and plastic strain was observed in the strain range 0.22 to 0.97.

3. The instability strain for this steel was about 90% of the true fracture strain. This is at variance with the theoretically derived strain $\varepsilon_i = 0.66$.

4. The estimated toughness $J_{1c} = 293 \ N/mm$ derived from tensile data was found to be close to the experimental values of J_{1c} obtained from the multiple specimens method, ASTM E 813-81.

REFERENCES

(1) Zheng, C.Q. and Radon, J.C (1983). Basic tensile properties of a low-alloy steel BS4360-50D. Proc. Conf. Fracture Mechanics Technology applied to material evaluation and structure design, Melbourne, Australia, J.C. Sih; N.E. Royan and R. Jones, Edts. M. Nijhoff, Publishers, The Hague, 243-256.

(2) Paris, P.C. et al (1979). Elastic-Plastic Fracture, ASTM STP 668, 5-36.

(3) Wei, Yu-Lin (1982). Application of Elastic Plastic Fracture Mechanics to a Steel in the ductile brittle transition region, M.Sc. Thesis, Imperial College.

(4) Kong, B. and Paris, P.C. (1979). Fracture Mechanics, ASTM STP 677, 770-780.

(5) Needleman, A. and Rice, J.R. (1978). Limits to ductility set by Plastic flow localization, Mechanics of Sheet Metal Forming, General Motors Research Laboratories, 237-267.

(6) Hutchinson, J.W. and Miles, J.P. (1974). J. Mech. Phys. Solids, 22, 61-71.

(7) Hahn, G.T. and Rosenfield, A.K. (1968). Applications of Related Phenomena in Titanium, ASTM STP 432, 5-32.

(8) Zheng, C.Q. and Radon, J.C. (1983). The formation of voids in the ductile fracture of a low alloy steel. Proc. ICF Int. Symp. on Fracture Mechanics (Beijing), Science Pres, Beijing, 1052-1056.

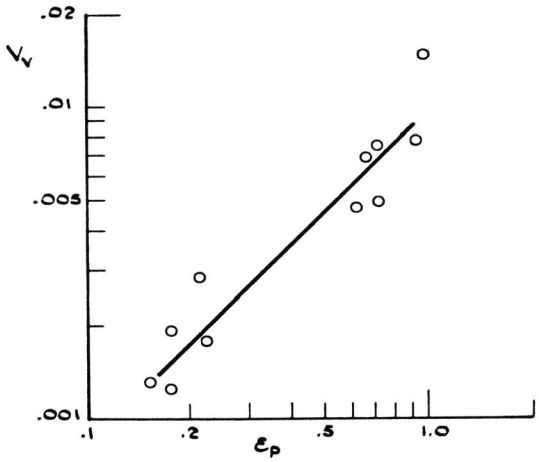

Fig. 3. Relative void volume V_v vs. plastic strain.

Fig. 1a. Spheroidal inclusion

Fig. 1b. Ellipsoidal void

Fig. 1c. Small inclusions

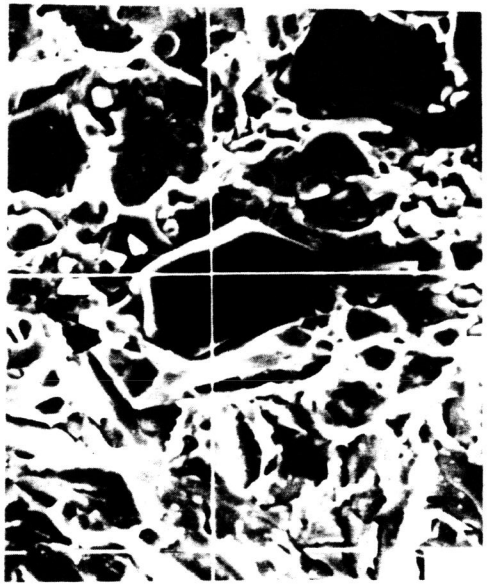

Fig. 2. Hexagonal particle